

NUMERICAL SIMULATIONS OF ALL OPTICAL SWITCHING IN NONLINEAR FBGS USING XPM AND SPM EFFECTS

Eubomír Scholtz, Libor Ladányi, Jarmila Müllerová

Institute of Aurel Stodola, Faculty of Electrical Engineering, University of Žilina,

ul. kpt. J. Nálepku 1390, 03101 Liptovský Mikuláš, Slovak Republic

Received 27 April 2016; accepted 6 May 2016

1. Introduction

All-optical signal processing, including the signal regeneration and wavelength conversion is very important for current and future ultra-high bit rate communications systems, since current electronic processing speeds are approaching fundamental limits near tens to hundreds of Gb/s. However, challenges still remain to improve device performance for practical applications [1]. Optical switching technologies have great impacts on the performance of the optical networks. Nowadays several technologies of optical switching already exist[2]. Each of them has some advantages and disadvantages. The most important performance parameter is the switching time. This parameter indicates the velocity of the change of the switched state. However, there are a lot of additional important parameters such as the insertion and polarization dependent losses, stability, scalability, energy consumption, crosstalk etc.

Devices based on nonlinear effects are capable to achieve short switching times. Nonlinear fiber Bragg grating (FBG) is a promising candidate for all-optical switching and processing in which the effect of nonlinear transmittance and/or optical bistability can be used for fast switching and controlling the switching behaviour of the grating. The combination of nonlinear material and distributed feedback in FBG results in the formation of optical bistability, where the output intensity can reach two values depending on the previous intensity. Optical bistability is a rapidly expanding field of current research because of its potential applications to all-optical logic and because of interesting phenomena it encompasses. Optical bistability has been observed in different optical devices and materials [3]. As appropriate the chalcogenide glasses appear. Chalcogenide glass offers many advantages as a platform both for fiber and integrated all optical devices due to the large Kerr nonlinearity, very low two-photon absorption and transparency from visible to IR region [1]

Due to optical bistability effect in FBG all-optical switching is possible. Switching in FBG means the change of the transmission state of the grating. Depending on the required options the switching can be completed by switching from the reflection to the transmission state of the grating (or vice-versa) what is possible by the Bragg wavelength shift caused by the change of the input intensity and therefore changing the detuning of the probe from the centre of the photonic band gap [4]. More options to achieve the wavelength shift exist. This can be realized by cross-phase modulation (XPM) of a strong pump and a weak probe or self-phase modulation (SPM) of a strong probe. Because of the obligation to have another control signal in XPM and due to similar power requirements of XPM and SPM the SPM-induced all-optical switching is more preferable. In self-switching the dynamic effects as the modulation instability (MI) are more pronounced and the necessity of optimization of these effects impacting temporal and spectral characteristics of the transported signal plays an important role.

2. Theory

An FBG with the input pump A_p , the probe wave A_0 and the notation used in the text below is illustrated in Fig. 4.

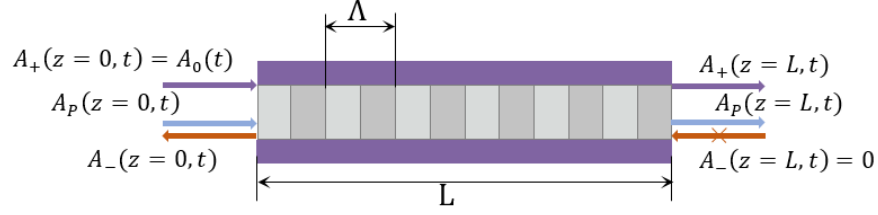


Fig. 4. Schematic illustration of the light propagation in FBG.

The set of nonlinear coupled mode equations (NLCMEs) to govern the nonlinear probe and pump wave propagations inside the nonlinear FBG [4,5] is given as

$$i \frac{\partial A_+}{\partial z} + i \frac{\bar{n}}{c} \frac{\partial A_+}{\partial t} + \delta A_+ + \kappa A_- + \Gamma_B (|A_+|^2 + 2|A_-|^2 + |A_p|^2) A_+ + F \Gamma_P (|A_p|^2) A_+ = 0 \quad (1)$$

$$-i \frac{\partial A_-}{\partial z} + i \frac{\bar{n}}{c} \frac{\partial A_-}{\partial t} + \delta A_- + \kappa A_+ + \Gamma_B (|A_-|^2 + 2|A_+|^2 + |A_p|^2) A_- + F \Gamma_P (|A_p|^2) A_- = 0 \quad (2)$$

$$i \frac{\partial A_p}{\partial z} + i \frac{\bar{n}}{c} \frac{\partial A_p}{\partial t} + \frac{1}{F} \Gamma_B (|A_+|^2 + 2|A_-|^2) A_p + \Gamma_P (|A_+|^2 + |A_-|^2 + |A_p|^2) A_p = 0 \quad (3)$$

where A_+ , A_- and A_p are the forward (+) probe, backward (-) probe and forward pump traveling wave functions, \bar{n} is the effective refractive index and $F = (\lambda_B/\lambda_p)$. δ is the detuning parameter, κ is the linear coupling coefficient, and $\Gamma_{B,P}$ are the nonlinear parameters defined as follows

$$\kappa(z) = \frac{\pi \Delta n(z)}{\lambda_B}, \quad \delta = 2\pi \bar{n} \left(\frac{1}{\lambda} - \frac{1}{\lambda_B} \right), \quad \Gamma_B = \frac{2\pi}{\lambda_B} n_2, \quad \Gamma_P = \frac{2\pi}{\lambda_p} n_2 \quad (4)$$

where $\Delta n(z)$ represents the modulation depth, n_2 is the nonlinear coefficient and $\lambda_B = 2\bar{n}\Lambda$ is the Bragg wavelength. λ_p is the wavelength of the pump. It is assumed that the pump propagates unchanged throughout the grating because its wavelength is far from the Bragg wavelength while the frequency of the probe lies within the photonic bandgap of the FBG.

3. Results

In our simulations $\text{Ge}_{10}\text{As}_{10}\text{Se}_{60}\text{Te}_{20}$ was selected as the third order nonlinear media. This material has the Kerr coefficient $n_2 = 20 \times 10^{-18} \text{ [m}^2/\text{W]}$ [6]. We simulated $\text{Ge}_{10}\text{As}_{10}\text{Se}_{60}\text{Te}_{20}$ as a periodic grating with the effective refractive index $\bar{n} = 2.9$. The characteristics of the grating were simulated with the parameters as follows: the grating length $L = 0.9 \text{ cm}$, the Bragg and probe wavelengths $\lambda_B = \lambda = 1550 \text{ nm}$, the pump wavelength $\lambda_p = 1500 \text{ nm}$ was selected far from the Bragg wavelength, the amplitude of the periodic index change Δn was selected to be 9×10^{-5} . The Gaussian pulses were simulated as input pulses.

The bistable behavior of the SPM ($I_p = 0, I_{max} = 200 \text{ MW/cm}^2$) and XPM ($I_p = 250 \text{ MW/cm}^2, I_{max} = 0.2 \text{ MW/cm}^2$) switching are depicted in Fig. 1. In case of SPM of strong input pulse the bistable behavior is clearly seen in the figure. If the pump signal for the switching is used the bistability disappears but the switching is still possible.

One possibility of signal switching is to use the bistability behavior for switching the solo pulses. This can be done with SPM using strong pulses. In Fig. 2 a) an input Gaussian pulse ($I_{max} = 200 \text{ MW/cm}^2, T_0 = 200 \text{ ps}$), transmitted and reflected pulses presented in the grating are depicted. The pulse passing through the grating causes a grating state change so that the grating is switched from the reflective to the transmissive mode. The transmitted pulse is compressed due to a part of pulse reflected from the grating because of lower intensities of rising and falling edges. The second option of solo pulses switching is via XPM. In case of low intensity input probe pulse ($I_{max} = 200 \text{ W/cm}^2, T_0 = 200 \text{ ps}$) this pulse can

be switched by its overlapping by a strong Gaussian pulse ($I_{P,max} = 230 \text{ MW/cm}^2, T_0 = 300 \text{ ps}$) as can be seen in Fig.2 b). If the pump pulse was not present the whole pulse was reflected from the grating. Hereby a long pump pulse can be used for overlapping the sequence of probe pulses for their switching in the grating.

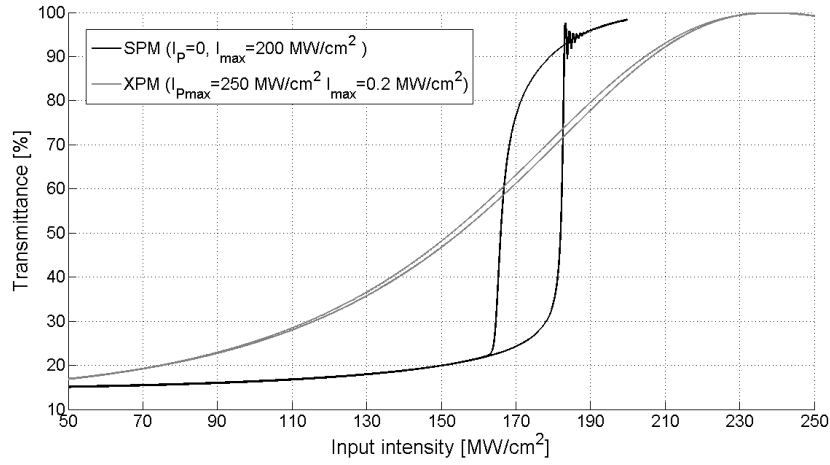
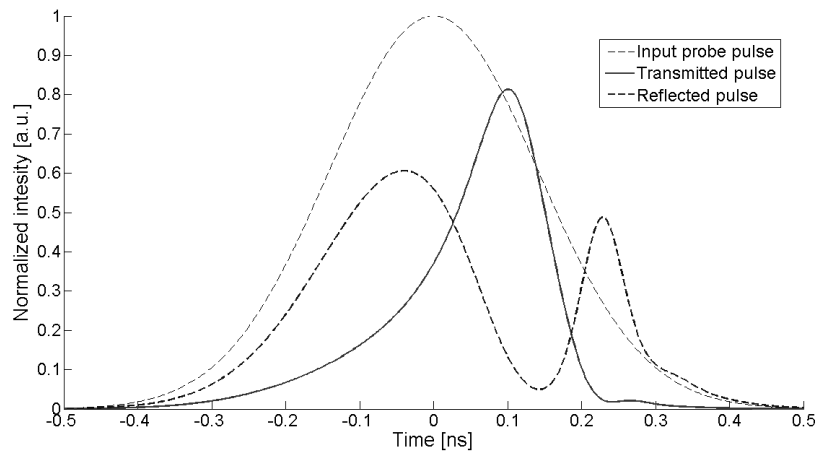
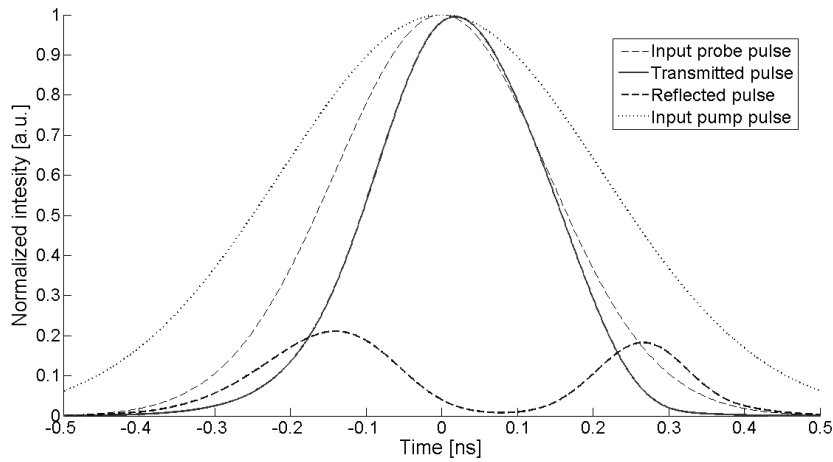


Fig.1: The bistable curve of $\text{Ge}_{10}\text{As}_{10}\text{Se}_{60}\text{Te}_{20}$ FBG in case of SPM and XPM effects.



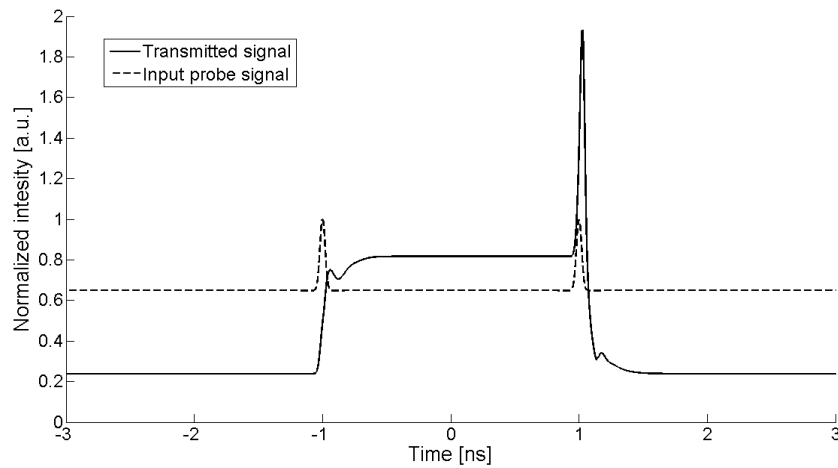
a)



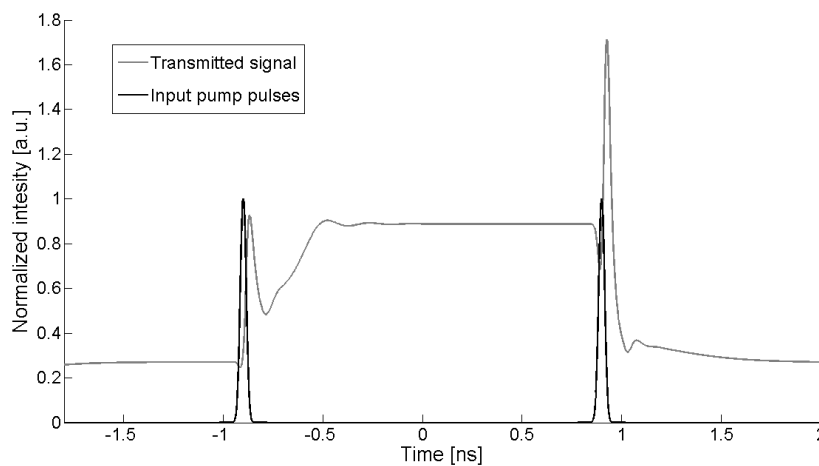
b)

Fig.2: The solo pulse switching using a) SPM and b) XPM effects.

The next possibility of SPM and XPM switching is using the short strong control pulses which cause the changes in the grating state. However in this case the probe intensity must lay in the middle of the bistable region. If the continuous wave (CW) signal is travelling through the grating with the intensity $I = 170 \text{ MW/cm}^2$ then a strong short pulse at the same wavelength carrier ($I_{max} = 10 \text{ MW/cm}^2, T_0 = 20 \text{ ps}$) causes the changes in the grating state from the reflective to the transmissive mode. The next strong input pulse causes an opposite grating state as depicted in Fig.3 a). Fig.3 b) depicts the similar situation where the CW probe signal passes through the grating but in this case the strong pump pulse can change the grating state. The first pump pulse with parameters $I_{max} = 100 \text{ MW/cm}^2, T_0 = 20 \text{ ps}$ causes the change of the grating state from the reflective to the transmissive mode and the second strong pump pulse causes the opposite grating state. The switching using the same strong pulse in both SPM and XPM is possible due to the peak compression followed by the longer dip in the probe transmission to satisfy the energy conservation laws after the strong pulse injection. As the energy conservation law is satisfied the probe transmission can decide whether to go to the high or the low state.



a)

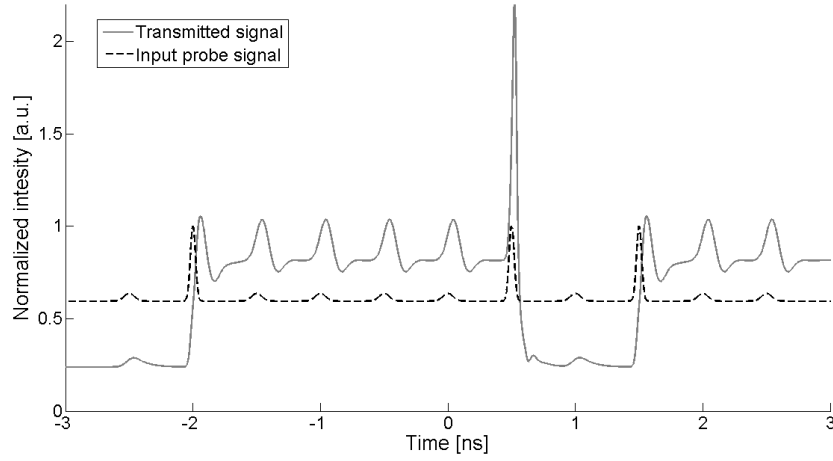


b)

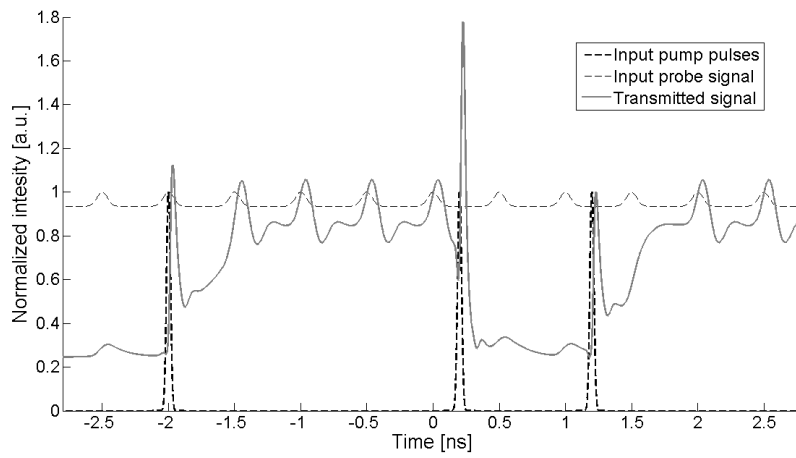
Fig.3: The continuous wave switching using a) SPM and b) XPM effects.

And hence the sequence of more pulses added to a CW signal with the necessary intensity lays in the middle of bistable region it can be controlled by the strong short pulses. Fig. 4 a) shows the possibility of switching using SPM where the pulses with $I_{max} = 0.2 \text{ MW/cm}^2, T_0 = 40 \text{ ps}$ are added to a CW signal with $I_{max} = 170 \text{ MW/cm}^2$ and three

pulses have $I_{max} = 10 \text{ MW/cm}^2$, $T_0 = 20 \text{ ps}$. Each of these three pulses causes a change in the grating state. If no stronger short pulse is present the grating reflects all of lower intensity pulses. If the first stronger pulse is present the grating switches from the reflective to the transmissive mode and starts to transfer all of 40 ps pulses until the next control pulse is present. A similar process is with using of short stronger pump pulses with $I_{p,max} = 100 \text{ MW/cm}^2$ and $T_0 = 20 \text{ ps}$. If the lower intensity pulses are added to a CW signal within the bistability regime the pulses sequence can be switched using a strong short pump as can be seen in Fig . 4 b). In both SPM and XPM switching there is the pulse degradation but on the other side there is the pulse amplification.



a)



b)

Fig.4: The pulses sequence switching using a) SPM and b) XPM effects.

4. Conclusion

In this paper, we introduced the possible application of a nonlinear FBG for all-optical switching. We showed several possibilities related to different types of switching via SPM and XPM effects. It was shown solo pulse switching using a strong probe pulse via SPM or using a lower intensity probe pulse switched by overlapping the strong pump via XPM. Moreover it was shown the controlling of the probe transmittance by a very short strong pulse with using SPM and XPM effects. Based on these simulations the similar power requirements can be observed. Each of these options appears to be used in all optical signal processing.

Acknowledgement

This work was supported by the Slovak Research and Development Agency under the project APVV-0025-12.

References:

- [1] V.G. Ta'eed, M.R.E. Lamot, D.J. Moss and B.J. Eggleton, *Opt. Express*, **14** (23), 11242 (2006).
- [2] M. Markovic, M. Solanska and M. Dado, In: *ELEKTRO 2014*, Rajecké Teplice, 68 (2014)
- [3] I. V. Kabakova, D. Grobnic, S. Mihailov, E. C. Magi, C. M. Sterke and B. J. Eggleton, *Opt. Express*, **19**(7), 5868 (2011)
- [4] Yosia , Shum Ping , Lu Chao, *Opt. Express*, **13**(13), 5127 (2005)
- [5] N. G. R Broderick, *Opt. Commun.*, **148**(1-3), 90 (1998)
- [6] S. Cherukulappurath, et al., *Opt. Commun.*, **242**, 313 (2004).